CHAPTER 5

DEVELOPMENT AND EVALUATION OF COENZYME Q10 LOADED LIPID-POLYMER HYBRID NANOPARTICLES

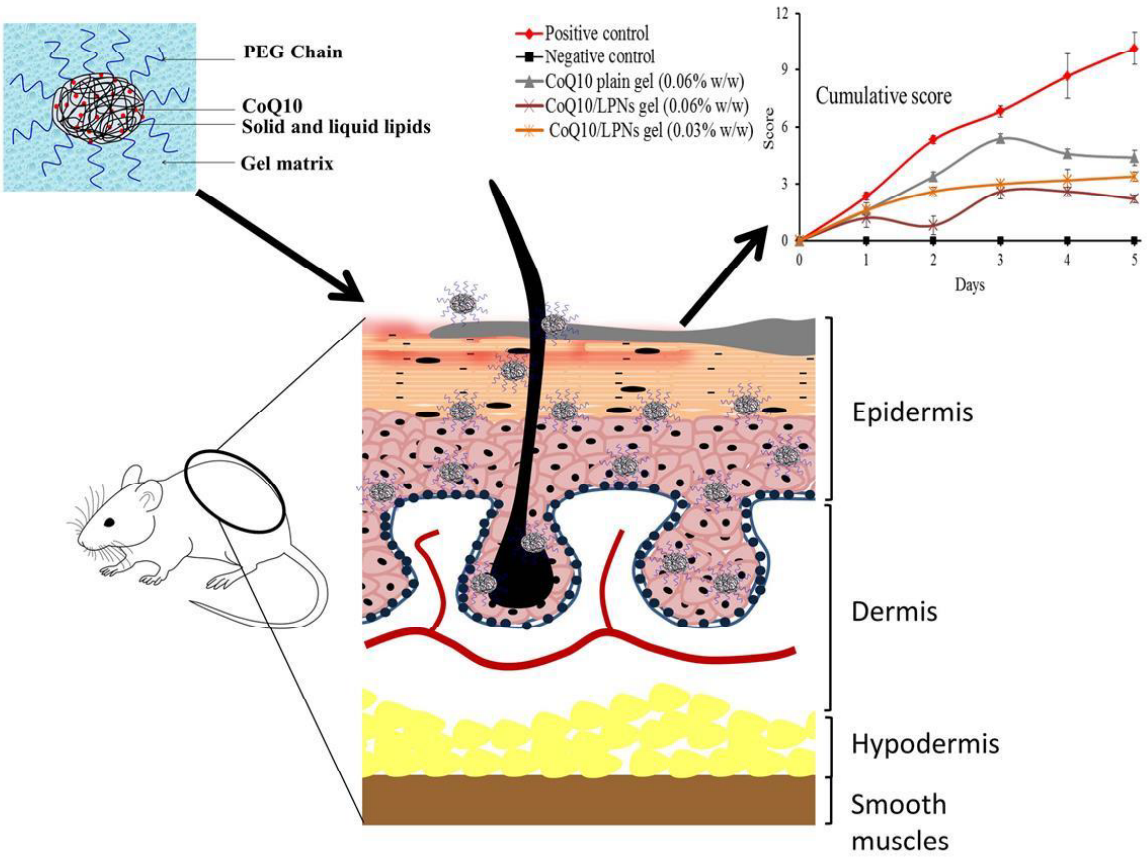

- **Introduction**
- **Experimental section**
- **Results**
- **Discussion**
- **Conclusion**

1. Introduction

Psoriasis is a chronic, autoimmune disease of skin affecting 2–3% of the population globally [1-9]. It is widely accepted that oxidative stress (OS) plays a major role in the pathogenesis of psoriasis. It mediates its damaging effect through several reactive oxygen species including hydroxyl radical, superoxide anion, hydrogen peroxide, and other oxygen-based free radicals resulting in DNA damage, lipid peroxidation, and induction of inflammatory cascade [10-14]. ROS stimulates several inflammatory signaling pathways mediated *via* mitogen-activated protein kinase (MAPK), nuclear factor-kB (NF-kB), and JAK-STAT signaling that has been reported to release inflammatory cytokines and vascular endothelial growth factor (VEGF) [15]. Further, it results in the activation of T-cell, keratinocyte proliferation and capillary proliferation (angiogenesis) at the affected site of skin, manifesting the immunopathological condition [15]. ROS can be generated either endogenously (*via* enzymes such as lipoxygenases, cyclooxygenases, myeloperoxidases and NADPH oxidases and during oxidative phosphorylation *via* electron transport chain (ETC)) or exogenously (heavy metals, UV radiation, and ischemia) [10]. The skin is equipped with several antioxidant defense systems, including enzymatic group (glutathione reductase, superoxide dismutases, catalase, metallothioneins, glutathione peroxidases, and thioredoxin/thioredoxin reductase system) and non-enzymatic group (reduced glutathione, α-tocopherol, ascorbic acid, and uric acid)) to counter damage associated with ROS [14]. There should be a proper balance between the level of the pro-oxidant and antioxidant defense system, ensuring the maintenance of skin barrier integrity. Inefficient detoxification or excessive generation of ROS leads to cellular dysfunctioning resulting in damage and manifestation of the inflammatory psoriatic disease [13]. It has been reported that oral administration of dimethylfumarate effectively ameliorate moderate

to severe type psoriasis by inducing NAD(P)H:quinone oxidoreductase 1 (NQO1) and glutathione, suggesting a well-developed antioxidant defense mechanism crucial for maintaining the integrity of skin and preventing damage associated with ROS [16].

Several topical preparations available for management of psoriasis are composed of retinoids, corticosteroids, salicylic acid, anthralin, coal tar and vitamin D analogues but are associated with side effects such as skin irritation, thinning of the skin, and dilated blood vessels and are not suitable from long term point of view [17-23]. To address the above challenges, research should be focused on developing such a therapy that should be free from side effects and should be applicable for long-term usage. Previously it was observed that antioxidants were effective in treating psoriatic condition [2, 13, 16, 24-29]. Coenzyme Q10 (ubiquinone or CoQ10) is an endogenous biomolecule localized in the mitochondria and plasma membrane of cells exerts a powerful antioxidant effect by directly detoxifying the generated ROS and thus protecting from cellular damage [30]. It exerts an anti-inflammatory effect by inhibiting various pathways such as NF-kB, Akt/mTOR, the receptor for advanced glycation end products (RAGE), extracellular signal-regulated kinase ½ (ERK ½) that are reported to be involved in the synthesis and release of pro-inflammatory cytokines [31-33]. It was also observed that oral supplementation of CoQ10 in psoriasis patients improved their disease condition [34]. Considering this, CoQ10 was selected for exploring its potential in psoriasis with the objective of designing safe therapy for long-term usage. Further, it was hypothesized that it would be beneficial to deliver this drug by topical route rather than oral because of the advantages of targeting drug directly to the site of interest. CoQ10 is highly lipophilic (log P of 10) and enforces challenges for topical delivery [35]. A new formulation of CoQ10 exhibiting deep skin penetration and possessing a prolonged release profile is desirable for obtaining maximum

benefits of this molecule. El-Leithy et al. reported 3.4 fold and 17.8 fold enhancement in the permeation of CoQ10 in rat skin when delivered as nanoemulsion based gel compared to its conventional products i.e. CoQ10 gel and CoQ10 cream, respectively, with resultant improvement in the anti-wrinkle efficacy [36-38]. Korkmaz et al. reported that the amount of CoQ10 permeated in rat skin was doubled when delivered as solid lipid nanoparticles compared to the free drug [39]. Another report provided by Gokce et al. concluded that antioxidant effects of CoQ10 against ROS were significantly improved when delivered as liposomes [40]. Lee et al. reported significant improvement in the topical penetration of CoQ10 when delivered as liposomes compared to its suspension [41]. There was a significant improvement in the *in vivo* anti-wrinkle efficacy of CoQ10 and retinaldehyde when delivered as nanostructured lipid carriers (NLCs) as reported previously by Nayak et al. [42]. Lipid-polymer hybrid nanocarriers are preferred over polymeric and lipidic nano-systems, which are associated with certain advantages and disadvantages over one another. This newer class of nanocarriers are featured with potential advantages such as enhanced cellular uptake, higher encapsulation efficiencies, a better controlled drug release profile with high biocompatibility [43].

This chapter outlines the development of monolithic lipid-polymer hybrid nanoparticles loaded with CoQ10 (CoQ10/LPNs) that consisted of a hydrophobic block of amphiphilic copolymer mixed uniformly with lipids (solid and liquid) forming hydrophobic core encapsulating hydrophobic drug i.e., CoQ10, whereas the hydrophilic block of amphiphilic copolymer forms a hydrophilic shell around the central core responsible for the colloidal stability of nanoparticles. The resulting CoQ10/LPNs were thoroughly characterized for the particle size distribution, morphological evaluation, and *in vitro* release mechanism. These CoQ10/LPNs

were further formulated into a topical gel using carbopol 974P as gelling agent followed by *in vivo* antipsoriatic efficacy testing using IMQ-induced psoriatic mouse model.

2. Experimental section

2.1. Materials

Coenzyme Q10 was purchased from Sisco Research Laboratories Pvt. Ltd (Mumbai, India). Amphiphilic copolymer; mPEG-PLA (molecular weight: 12927 Da) was synthesized in house using our previously reported procedure [44]. D,L-lactide (DL-LA), methoxy poly(ethylene glycol) (mPEG, Mn 5000), and stannous 2-ethyl hexanoate (Sn(Oct)2) were purchased from Sigma Aldrich (St. Louis, MO). Labrasol® and Precirol® ATO5 were received as gift sample from Gattefosse, (Lyon, France). Linoleic acid was copped from Acme Synthetic Chemicals, (Mumbai, India). Tween 80 was received as a gift from BASF India Ltd, (Mumbai, India). Phosphate Buffered Saline (PBS) pH 7.4 was procured from HiMedia Laboratories (Mumbai, India). Carbopol 974P was obtained as a kind gift from Lubrizol, (OH, USA). Commercially available topical cream of imiquimod (Imiquad®, 5% w/w) was procured from Glenmark, (Mumbai, India). All other chemicals and reagents (analytical grade) were purchased from local vendors. Purified water was used throughout the studies (Millipore, Bedford, USA).

2.2. Formulation development

2.2.1. Preparation and characterization of CoQ10 loaded lipid-polymer hybrid nanoparticles (CoQ10/LPNs)

The method given in chapter 4 was adopted for the preparation of CoQ10 loaded LPNs. Briefly, CoQ10 (20 mg), Precirol®ATO 5 (180 mg), linoleic acid (180 mg) and mPEG-PLA

(180 mg; molecular weight: 12927 Da) were transferred to a 25 mL round-bottomed flask (RBF) and were dissolved in chloroform (800 μL) by slight warming at 40 ºC. Chloroform was removed under vacuum using a rotary evaporator (Buchi Rotavapor® R-300, Switzerland) to form a uniform hybrid matrix film which was later dispersed in 10 ml of an aqueous solution containing tween 80 (1.5% w/v) (pre-heated to 60°C) and was transferred to 15 ml glass vial. The crude dispersion was subjected to probe sonication at 20% amplitude for 2 min at 60°C. The hot nanodispersion was immediately cooled on an ice bath followed by centrifugation at 5000 rpm for 5 min to remove the unentrapped CoQ10. The supernatant containing nanoparticles was collected and analyzed for particle size and zeta potential using Malvern Zetasizer (Malvern Nano ZS). For particle size and size distribution analysis, sample was prepared by diluting formulation 20 times with Milli-Q water and for zeta potential measurements, samples were analyzed undiluted. Percent encapsulation efficiency (% EE) of the drug was determined using reverse-phase high-pressure liquid chromatography (RP-HPLC) analytical using our developed methas given in chapter 2. Percent encapsulation efficiency (% EE) was calculated using following equation:

$$\% \text{ EE} = (\text{Amount of drug in LPNs} / \text{Initial amount of drug taken}) \times 100$$

The morphological examination of developed nanoparticles was carried out by using FE-SEM (FEI Quanta FEG 250 SEM, Hillsboro, Oregon, Washington).

2.2.2. *In vitro* drug release study and release kinetics

In order to investigate drug release of CoQ10 from LPNs, a destructive sampling technique was followed as dialysis bag was acting as barrier for drug release. Briefly, nanoparticles (CoQ10 equivalent to 431 µg; 100 µL) were dispersed in 900 µL of release media (consisting of Labrasol

(5% w/v) in phosphate buffer saline of pH 7.4 to maintain sink condition) in eppendorf tubes (2 mL) and placed in an incubator shaker maintained at 37ºC/300 rpm. At pre-decided time intervals (i.e., 0.25 h, 0.5 h, 1 h, 2 h, 4 h, 8 h, 12 h, 1 day, 2 day, and 3 day), the eppendorf tubes were ultracentrifuged (Sorvall™ MX Plus Series Floor Model Micro-Ultracentrifuge, Thermo Scientific™, Mumbai, India) for 1 h 10 min at 1,40,000 rpm/25°C and the quantity of drug in the supernatant was determined using RP-HPLC and percent cumulative drug release was plotted against time. Free CoQ10 at equivalent quantities was kept as a control for comparison purpose. At the end of the experiment, the drug release mechanism from LPNs was determined by fitting the data in different kinetic models and obtaining best fit from the values of correlation coefficient (R^2) and Akaike information criterion (AIC) by using DDSolver software (an add-in program).

2.2.3. Preparation and characterization of gel containing CoQ10/LPNs

A topical gel containing CoQ10/LPNs (~15 mg of CoQ10; 25 g) was prepared using carbopol 974P (0.75% w/v) as gelling agent. Carbopol 974P (0.1875 g) was transferred to a tared beaker and allowed to hydrate overnight by adding purified water (5 ml) followed by addition of CoQ10/LPNs (~15 mg of CoQ10) and mixed until homogeneous. Later, propylene glycol (3.25 g), propylparaben (0.075 g) and methylparaben (0.075 g) were added to the above mixture and were subjected to vigorous stirring using a glass rod until a visually uniform product was obtained. This was followed by the addition of purified water to adjust the weight to 25 g, and pH of the resulting mixture was brought to 6.8 by using 1 M NaOH, which neutralizes the acidic functional group of carbopol and produces viscous gel. Blank LPNs, CoQ10/LPNs and their corresponding gels were lyophilized (FreeZone Triad® Benchtop Freeze Dryers (Labconco, MO, USA)) followed by their characterization using FT-IR (Bruker Apha, MA, USA) and DSC

(DSC-60 Plus Shimadzu, Kyoto, Japan). Further, the rheological studies of the CoQ10/LPNs gel were carried out using a Rheometer (MCR 92, Anton Paar, Germany) as reported previously [44]. Furthermore, the behavior of viscosity of final product with rise in temperature was examined. In addition to these, oscillatory rheological tests, including amplitude sweep test and frequency sweep test, were carried out at 25 °C with a 0.2 mm gap. Primarily, an amplitude sweep test was conducted on the sample to define the linear viscoelastic (LVE) region at a fixed frequency of 10 rad/s, a strain (γ) varying from 1 to 100%. Subsequently, the frequency sweep test of gel was carried out in the frequency range 0.1–100 rad/s by subjecting to deformation within the LVE region, and the physical stability of the gel was predicted.

2.3. *In-vivo* antipsoriatic efficacy studies

2.3.1. Design of study protocol and establishment of IMQ-induced plaque psoriatic mouse model

To evaluate in vivo efficacy of developed CoQ10 containing formulations, we used our previously reported IMQ-induced plaque psoriatic mouse model [44]. IMQ is a TLR7/8 receptor ligand and acts as potent immune stimulator which can be used topically to induce and exacerbate psoriasis like dermatological condition with clinical relevance [29, 45-47]. Adult female Swiss albino mice (10-12 weeks) were obtained from Central Animal Facility BITS Pilani (Rajasthan, India). All the experimental procedures were carried out according to principles of CPCSEA guidelines and were approved by Institutional Animal Ethics Committee, (IAEC) (protocol no: IAEC/RES/25/11). Animals were allowed to acclimatize in pathogen-free environment for one week at 23 ± 1°C and 12-12 h dark-light cycle prior to the actual experiment and provided with food and water ad libitum. Healthy disease-free mice were trimmed on their backs, and remaining hairs were removed using Veet (Cedex, France) and

subsequently divided into five groups (n=6): Group 1 (Negative control (kept without any treatment: IMQ or test product)), Group 2 (Positive control (treated with only IMQ but no test product)), Group 3 (CoQ10 gel (0.06% w/w)), Group 4 (Test product, CoQ10/LPNs gel (0.03% w/w)) and Group 5 (Test product, CoQ10/LPNs gel (0.06%w/w)). Animals from groups 2-5 were subjected to topical treatment with 62.5 mg of commercial IMQ cream (5% w/w) onto their right ear and shaved back for 5 consecutive days [44]. Group 3-5 were treated with CoQ10 containing formulations at a dose of 40 mg/cm^2 whereas the negative control group was not subjected to any treatment (either IMQ or CoQ10 formulation) and served as healthy animals (Figure 5.4).

2.3.2. Evaluation of changes in Psoriasis Area Severity Index (PASI)

To score the extent of inflammation of back skin and right ear, a scoring system based on the clinical Psoriasis Area and Severity Index (PASI) was adopted where psoriatic parameters such as erythema, scaling, thickening were scored independently by two personnel on a scale from 0-4: none (0), slight (1), moderate (2), marked (3), very marked (4). Additionally, cumulative scoring (sum of scaling plus erythema plus thickening) was measured on a scale from 0 to 12 and designated the severity of induced psoriatic inflammation. Measurement of back skin thickness and ear thickness (both left (control; no treatment) and right) were done using digital vernier caliper and micrometer. An increase in the thickness of the back skin and right ear were directly correlated to the severity of psoriasis. At the end of the study duration on Day 5, animals from all the groups were sacrificed and spleens were isolated from comparing their size and average weights. The changes in their sizes and weights were correlated to the dynamic body changes. Additionally, percent change in body weights of animals during the entire study duration from

Day 0 to Day 5 was measured and the degree of change in their values was directly linked to the efficacy of treatment and recovery to animals to normal or healthy state.

2.3.3. Histopathology and immunohistochemistry (IHC)

At the end of study (Day 5), various tissues such as back skin (BS), right ear (ES), spleen and liver were isolated after sacrification of animals and examined histopathologically by Eosin and Hematoxylin staining for the degree of damage. Skin samples (both ES and BS), were evaluated for the potential parameters resulting in dermal damage that includes parakeratosis, hyperkeratosis, angiogenesis, epidermal hyperplasia, inflammatory infiltrates, suprapapillary thinning, pustule of Kogoj, munro's microabscess, and the resultant total skin damage score (cumulative score consisting of the sum of all the above parameters). Parameters leading to liver damage that includes inflammatory infiltrates, hepatocyte degeneration, and their cumulative score i.e. total liver damage score was examined. In case of spleen samples, parameters such as integrity of speenocyte and depopulation of lymphocytes and their resultant total spleen damage score was determined.

Further, immunohistochemistry of Ki-67 (an indicator of cell proliferation expressed in back skin), was studied for all the groups and result was reported as the average number of Ki67 positive cells stained per high power field which was an index of cellular proliferation and hence the extent of induced psoriasis [48-53].

2.3.4. ROS scavenging efficacy

The *in vivo* ROS scavenging efficacy was evaluated on the basis of malondialdehyde (MDA) and reduced glutathione (GSH) levels expressed in the psoriatic back skin of mice of various treatment groups. The principle of detection of these biological markers was based on

simple colorimetric assays. Briefly, the procedure compromised of preparation of skin homogenate in lysis buffer using high shear homogenizer followed by estimation of total protein content by biuret test. This was followed by estimation of malondialdehyde (MDA) and reduced glutathione (GSH) levels by Wills and Ellman method, respectively, as reported earlier with slight modification [55, 56]. For MDA determination, 100 µL of skin homogenate was mixed with 750 µL (20% v/v glacial acetic acid), 100 µL (8.1% w/v aqueous sodium dodecyl sulphate (SDS) solution), 750 µL (0.8% w/v aqueous thiobarbituric acid (TBA) solution) and resulting contents were heated at 95°C for 1 h. Further, the contents were centrifuged at 10000 rpm for 10 min and supernatant was isolated and checked for MDA levels at 532 nm using spectrophotometer (Epoch microplate spectrophotometer, BioTek instruments, U.S.). The values were represented as micromole per gram of protein. For GSH determination, 100 µL of skin homogenate was mixed with 100 µL (5% w/v sulphosalicylic acid) and kept at 4°C for 1 h. Further, the contents were centrifuged at 10000 rpm for 10 min and 100 µL of supernatant was mixed with 450 µL of phosphate buffer and 1.5 mL of 1% w/v solution of 5,5-dithiobis-(2-nitrobenzoic acid) (DTNB) in 0.1 M phosphate buffer (pH 8) and incubated for 10 min at 37°C. The absorbance of contents were checked at 412 nm using spectrophotometer and the values were expressed in µg/mg of protein.

2.4. Statistical analysis

Analyses were carried out using GraphPad Prism (GraphPad Software (version 8), La Jolla, CA, USA). All the quantitative data are presented as mean ± standard deviation (SD) or standard error of the mean (SEM) and significant differences between two or more treatment

groups were determined with analysis of variance (ANOVA) followed by Tukey's test wherein p-value ≤ 0.05 was considered statistically significant.

3. Results

3.1. Characterization of CoQ10/LPNs and CoQ10/LPNs gel

The CoQ10/LPNs showed smaller particle size (121 ± 11.61 nm), narrow PDI (0.252 ± 0.073), zeta potential (-20.23 ± 6.67 mV) and encapsulation (78.57 ± 3.88%) Figure 5.1(A). The

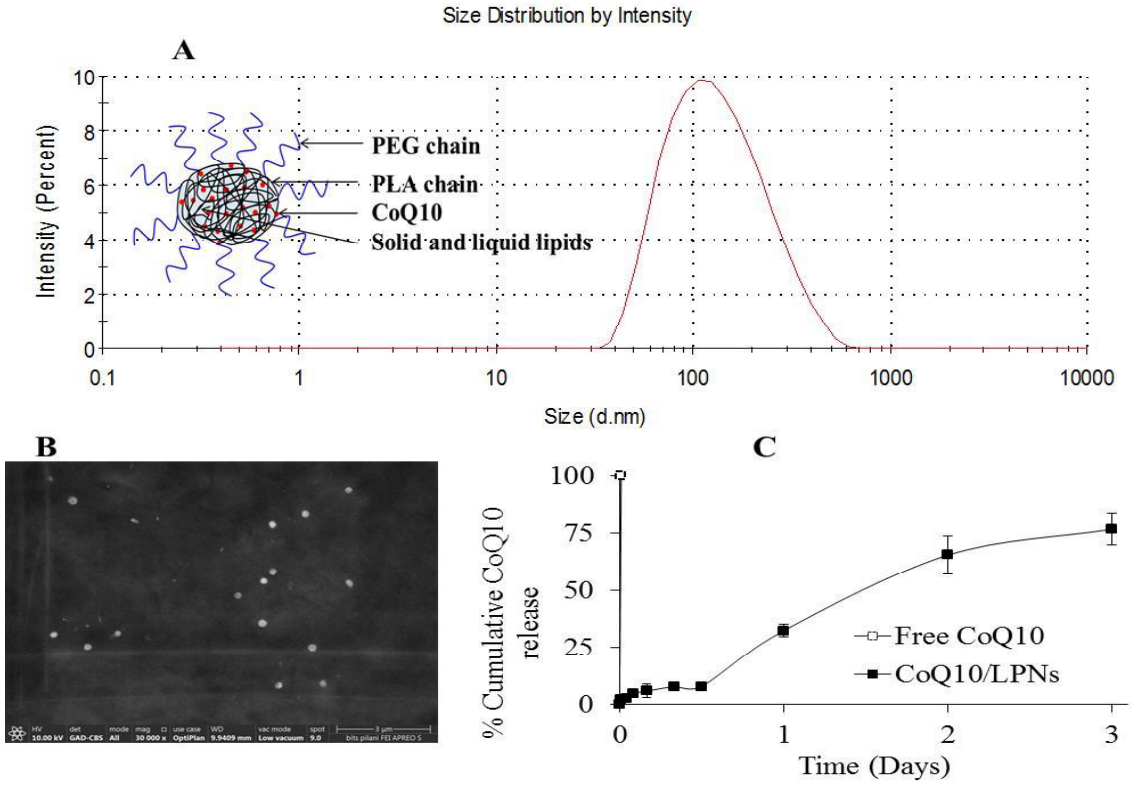

Figure 5.1. Physicochemical characterization of monolithic CoQ10 loaded polymer-lipid hybrid nano-carrier (CoQ10/LPNs). (A) Schematic representation of CoQ10/LPNs along with the particle size distribution demonstrating unimodal size distribution with mean hydrodynamic diameter of 121 nm and polydispersity index of 0.252 determined by dynamic light scattering (Malvern Nano ZS), (B) FE-SEM image showing uniform and spherical morphology, (C) In vitro drug release profile of CoQ10 from CoQ10/LPNs exhibiting sustained drug release without any burst release (n = 3, Mean ± SD).

developed CoQ10/LPNs demonstrated uniform and spherical morphology evident from FE-SEM images Figure 5.1(B). In-vitro sustained drug release profile for CoQ10/LPNs is depicted in

Figure 5.1(C), exhibiting cumulative release of 76.76 ± 6.87% at the end of day 3, whereas free CoQ10 showed complete dissolution within 15 min. Various kinetic model, including Higuchi, First-order, Zero-order, Hixson-Crowell, and Korsemeyer-Peppas were applied to the release data. The release of CoQ10 from the LPNs was best fitted in Hixson-Crowell model (R^2:0.9749 and AIC:53.9662) while the n-values (n = 0.916) acquired from the Korsmeyer–

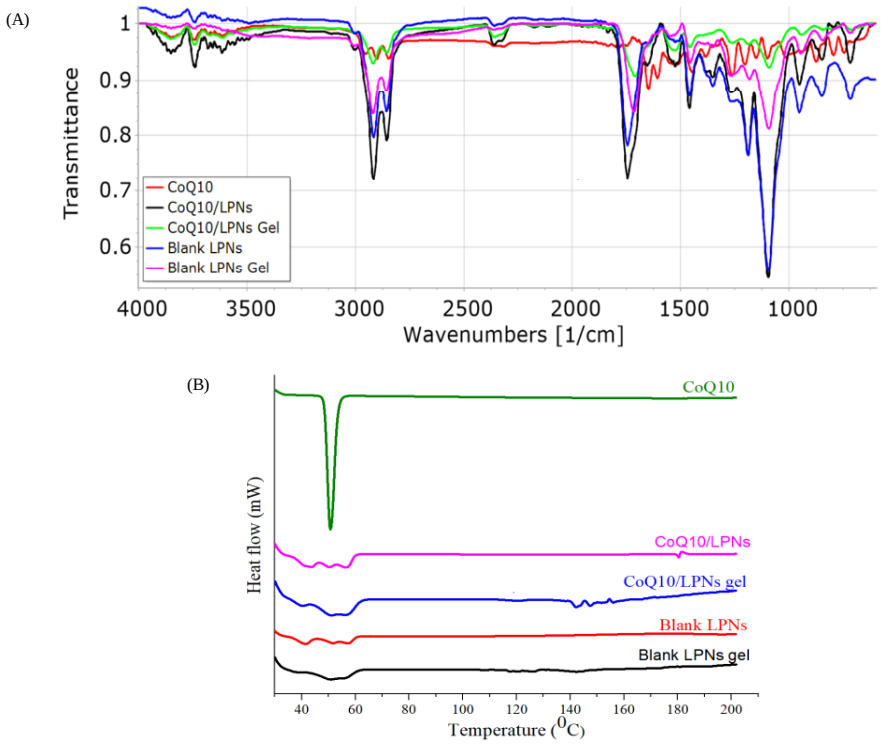

Figure 5.2. (A) FT-IR spectra of CoQ10, CoQ10/LPNs, CoQ10/LPNs gel, blank LPNs and blank LPNs gel and (B) DSC thermograms of CoQ10, CoQ10/LPNs and CoQ10/LPNs gel, blank LPNs and blank LPNs gel.

Peppas model indicated the mechanism of drug release followed non-fickian diffusion or anomalous diffusion. As shown in Figure 5.2(A), the FT-IR spectrum of CoQ10 showed its

typical peaks at 3281 cm^{-1} (O-H stretch), 2939 cm^{-1} (CH_3 asymmetric stretching), 2872 cm^{-1} (CH_2 symmetric stretching), 1518 cm^{-1} (C=C stretch). FT-IR spectrum of CoQ10/LPNs and

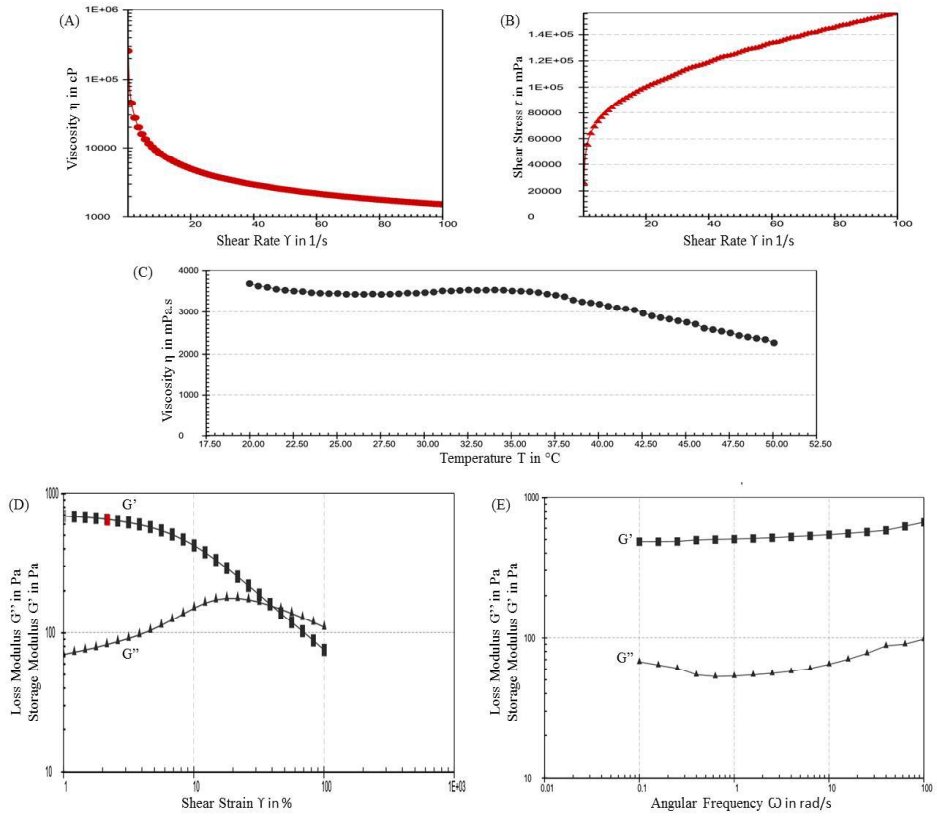

Figure 5.3. Rheological measurements and oscillatory rheological analysis of CoQ10/LPNs gel indicated non-newtonian type system with pseudoplastic properties and variable thixotropy (A) Viscosity (η) against shear rate (1/s) and (B) shear stress against shear rate (1/s) graphs, (C) stability of gel 3D matrix evident from the graph of viscosity (η) against temperature (°C) demonstrating no sudden collapse of viscosity (mPa.s) with rise in temperature (°C), (D) amplitude sweep test data indicating viscoelastic gel formation with G' > G" within the linear viscoelastic (LVE) region wherein G' is storage modulus and G" is loss modulus, (E) frequency sweep test data suggesting long term storage stability as obvious from higher storage modulus than loss modulus (G' > G") in lower frequency region.

CoQ10/LPNs gel revealed the absence of most of these characteristic drug peaks, which could be due to the loading of active into the nanoparticles core and lower drug/feed material ratio.

Furthermore, the FT-IR spectrum of CoQ10/LPNs gel and CoQ10/LPNs did not differ significantly from blank LPNs gel and blank LPNs, respectively. It was evident from the FT-IR spectra that in the case of blank LPNs gel and CoQ10/LPNs gel, there was a slight reduction in the intensity of peaks in comparison to the blank LPNs and CoQ10/LPNs, respectively signifying interaction between the nanoparticles and gelling agent (carbopol). A sharp endothermic peak corresponding to the melting point of CoQ10 was detected at 86 °C in the DSC thermogram of CoQ10, indicating its crystallinity Figure 5.2(B). However, the DSC thermogram of CoQ10/LPNs and CoQ10/LPNs gel revealed the absence of melting point of drug, indicating its conversion to amorphous form after loading into the nanoparticles. Viscocity (η) of CoQ10/LPNs gel was found to be 13159 mPa.s characterized by the pseudoplastic system with variable thixotropy obvious from graphs of shear stress against shear rate and viscosity against shear rate Figure 5.3.

3.2.*In vivo* antipsoriatic efficacy studies

3.2.1. Psoriasis Area Severity Index (PASI) evaluation

As shown in Figure 5.5, in group 2 (positive control), all the PASI parameters (erythema, scaling, thickening and cumulative score) progressively increased significantly from Day 1 to Day 5. It was clearly demonstrated that all the three groups treated with CoQ10 containing formulations: Group 3, 4 and 5 were able to comparatively reduce the scores of the above-mentioned parameters out of which group 5 treated with CoQ10/LPNs gel (0.06% w/w) gave the best results. Group 4 that was treated with CoQ10/LPNs gel (0.03% w/w) showed improved efficacy as compared to Group 3 treated with free CoQ10 gel (0.06% w/w), demonstrating enhanced efficacy.

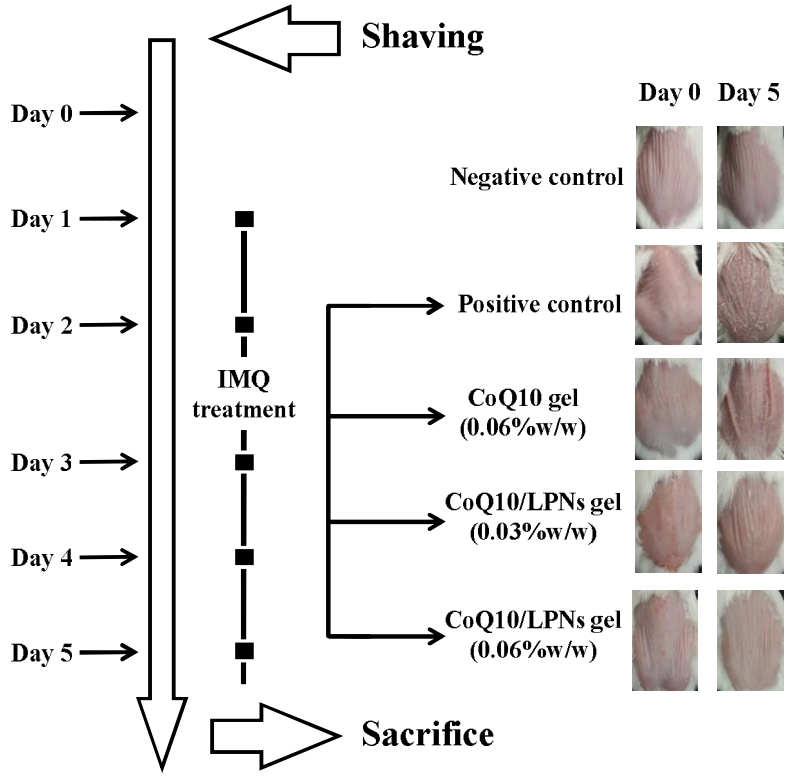

Figure 5.4. Schematic representation of study protocol for conducting IMQ-induced in vivo anti-psoriatic efficacy studies along with representative photographic presentation of back skin of animals from various groups on day 0 and day 5.

3.2.2. Measurement of back skin and ear thickness

There was a prominent rise in the back skin and right ear thickness (left ear served as control (without treatment)), upon topical application of IMQ due to keratinocyte hyperplasia stimulated by underlying inflammation in the positive control group. Reducing the thickness to normal or inhibiting the increase in the thickness dictated the efficiency of treatment. The average back skin thickness (mm) on day 5 for positive control, free CoQ10 gel (0.06% w/w), CoQ10/LPNs gel (0.03% w/w) and CoQ10/LPNs gel (0.06% w/w) groups were 2.466, 1.742, 1.610 and 1.482 respectively whereas the average right ear thickness (mm) for the above groups

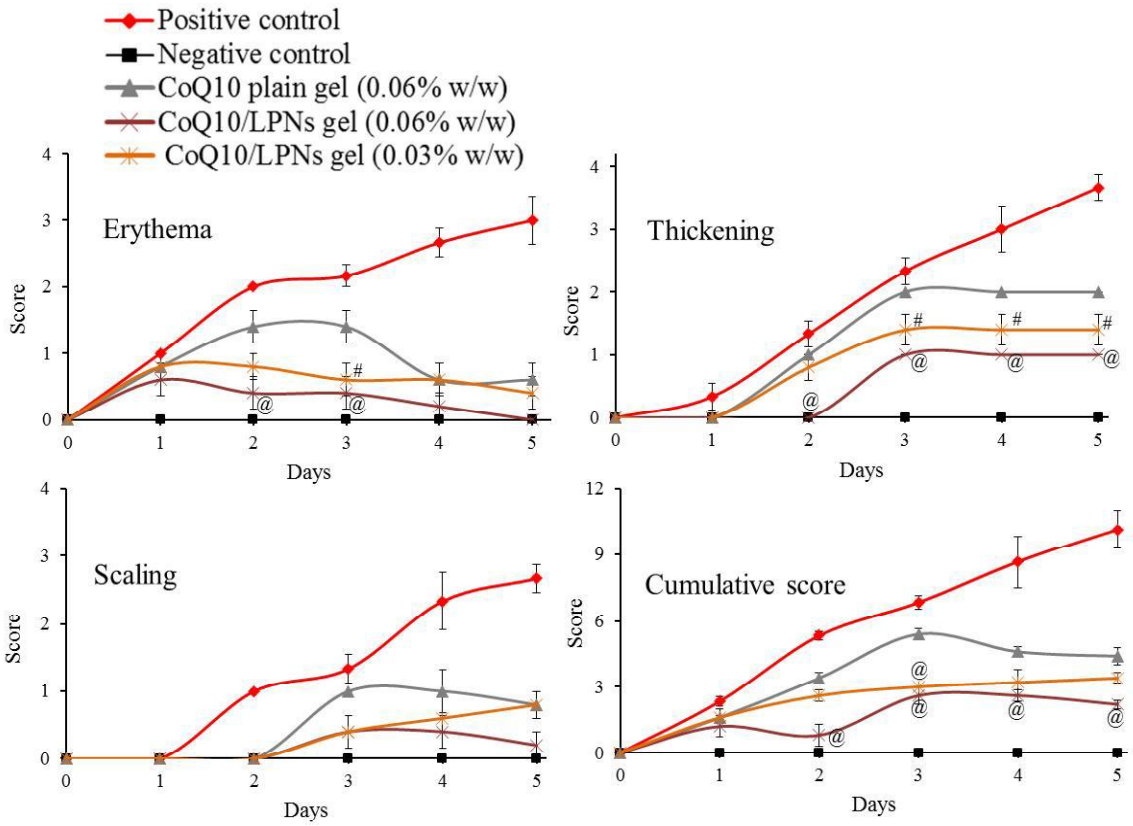

Figure 5.5. CoQ10/LPNs gel reduces the PASI scores and ameliorated the skin lesion of IMQ-induced plaque psoriatic mouse model in Swiss albino mice (n = 6). Antipsoriatic efficacy was evaluated based on PASI scores measured on a scale from 0 to 4 for parameters (erythema, scaling, and thickening) and from 0 to 12 for cumulative score (summation of erythema + scaling + thickening) which served as an index of extent of psoriasis induced. Data is presented as mean ± SEM. #, $p \leq 0.05$ and @, $p \leq 0.01$, versus CoQ10 gel (0.06% w/w) treated group.

sequence were 0.345, 0.309, 0.305 and 0.290 mm, respectively Figure 5.6. From the results, it is clear that there is an improvement in the efficacy of CoQ10 when it is delivered as LPNs gel compared to plain gel.

3.2.3. Measurement of average spleen weights and percent change in body weights

Spleen is highly sensitive to the level of inflammation, and several reports have concluded that the topical application of IMQ onto back skin results in splenomegaly. At the end

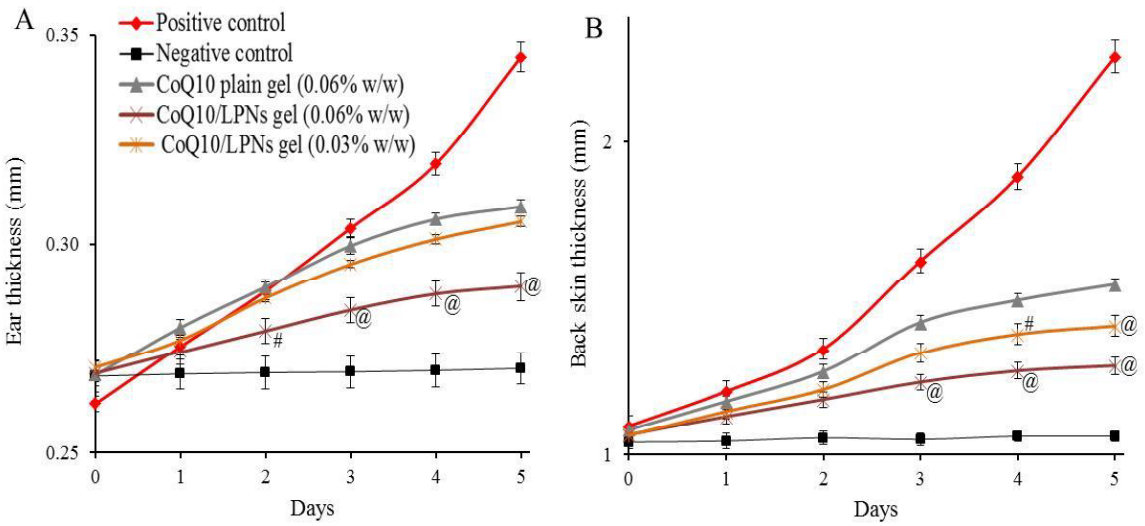

Figure 5.6: CoQ10/LPNs gel substantially inhibited the rise in skin thickness induced by topical application of IMQ. Commercial product of IMQ (Imiquad® (5% w/w)) was applied topically onto the right ear and back skin of Swiss albino mice for 5 consecutive days and resulted into thickening of the skin tissue due to underlying dermal inflammatory cascade accompanied by hyperplasia of keratinocytes. Bringing back the thickness to normal or suppressing the rise in the thickness marked the efficiency of treatment. Measurement of the (A) average right ear thickness and (B) average back skin thickness for various groups using digital micrometer and vernier caliper on the indicated days. Symbols represented average thickness ± SEM (n = 6). Data is presented as mean ± SEM. #, $p \leq 0.05$ and @, $p \leq 0.01$, versus CoQ10 gel (0.06% w/w) treated group.

of the study, animals were sacrificed, and spleens were isolated and compared for their size and average weights. Treatment with IMQ in the positive control group induced severe inflammatory condition resulting in an increase in the average weight of the spleen to 305 mg. The average weight of spleen for groups treated with free CoQ10 gel (0.06% w/w), CoQ10/LPNs gel (0.03% w/w) and CoQ10/LPNs gel (0.06% w/w) were found to be 180, 156, and 128 mg, respectively Figure 5.7(A). During the study period, the body weights of animals were measured to check the extent of fluctuation in their weights and/or their noticeable reduction at the end of the study on day 5. It was observed that the negative control group did not show any weight variation with no

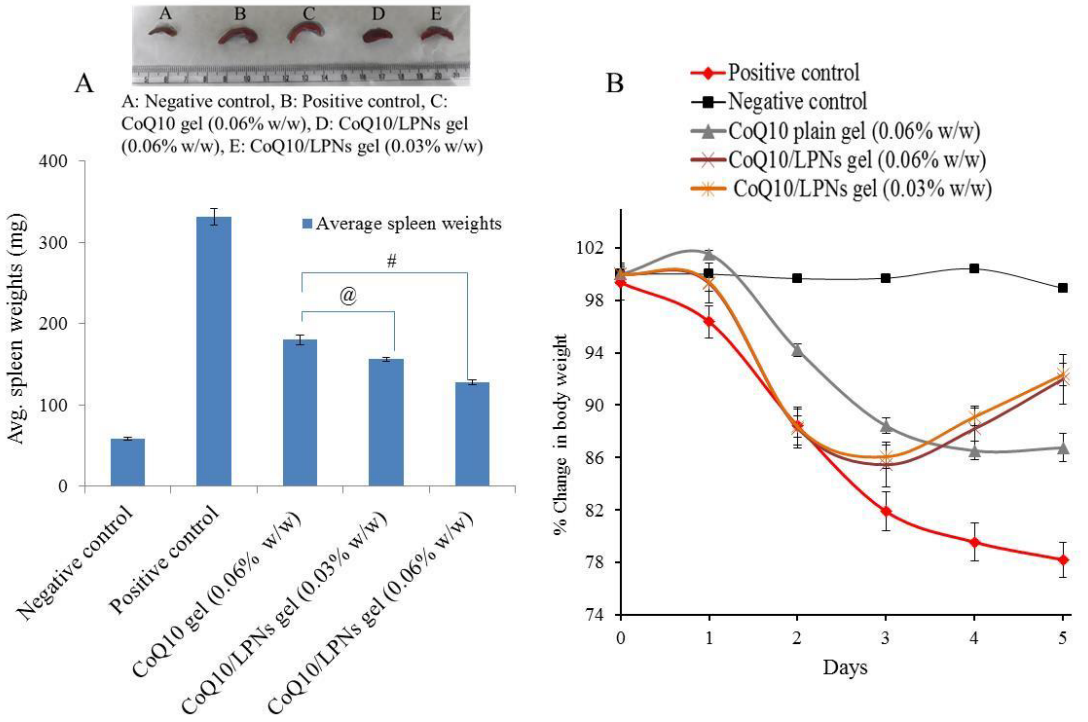

Figure 5.7. Topical application of IMQ exhibited toxicity by inducing splenomegaly and body weight fluctuation (reduced body weights). CoQ10/LPNs gel showed improved recovery w.r.t. both spleen weights and body weights. (A) Average spleen weights of various treatment groups, along with their comparative spleen sizes viz. (a) negative control, (b) positive control, (c) CoQ10 gel (0.06% w/w), (d) CoQ10/LPNs gel (0.03% w/w), (e) CoQ10/LPNs gel (0.06% w/w) and (B) percent change in body weight indicating improved recovery in groups treated with CoQ10/LPNs gel on Day 5. Data is presented as mean ± SEM. #, $p \leq 0.05$ and @, $p \leq 0.01$, versus CoQ10 gel (0.06% w/w) treated group.

significant difference between the average weights of animals on Day 0 and Day 5, indicating the healthy state of animals. In the case of the positive control group, there was significant fluctuation observed in weights of animals with a reduction in their values to 78% on day 5. The weights of animals from various groups i.e. free CoQ10 gel (0.06% w/w), CoQ10/LPNs gel (0.03% w/w) and CoQ10/LPNs gel (0.06% w/w) were reduced to 86, 92 and 91% respectively on day 5 Figure 5.7(B).

3.2.4. Histopathology and immunohistochemistry (IHC)

Apart from topical induction of psoriasis-like skin inflammation resembling clinical psoriasis, topical application of IMQ results into liver and spleen toxicity. The efficiency of an ideal treatment should reduce these additional toxicities apart from mitigating the dermal psoriatic state. Figure 5.8 shows histopathological sections of various tissues (right ear (ES), back skin (BS), liver, and spleen) stained by Hematoxylin and Eosin (H&E). In the positive control group subjected to only IMQ treatment, H&E analysis of both right ear and back skin demonstrated the presence of rete ridges (marked in red color circle) and hyperkeratosis that are reported as a hallmark of psoriasis and proved successful development of a psoriatic model. In addition to these parameters, positive control samples were characterized by marked acanthosis (epidermal thickening) due to hyperproliferation of basal and suprabasal keratinocyte involving significant inflammation. Total skin damage score (sum of all the individual scores of psoriatic skin parameters i.e. parakeratosis, hyperkeratosis, epidermal hyperplasia, angiogenesis, suprapapillary thinning, inflammatory infiltrates, pustule of Kogoj and munro microabscess) was considered for evaluating various groups. Total skin damage score of both ES and BS for positive control, CoQ10 gel (0.06% w/w), CoQ10/LPNs gel (0.03% w/w) and CoQ10/LPNs gel (0.06% w/w) were found to be 15, 8, 4, 1 and 14, 8, 4, 1 respectively suggesting significant improvement in LPNs treated group Table 5.1.

The association of IMQ induced plaque psoriatic mouse model and liver toxicity was previously established. H&E analysis of the liver section of positive control group demonstrated infiltration of inflammatory cells from the central vein with additional degeneration of hepatocyte resulting in liver damage with the highest liver damage score of 5. Total liver damage

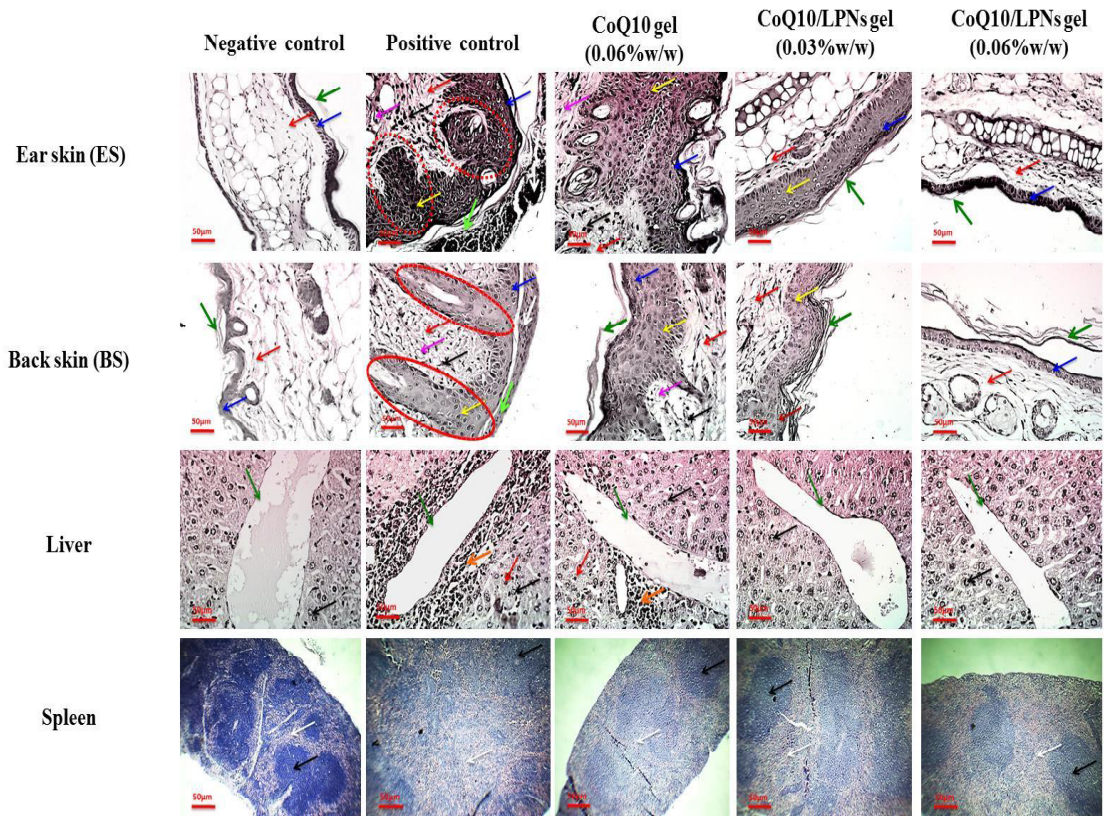

Figure 5.8. Comparative histological alterations in various tissues such as right ear skin (ES), back skin (BS), liver and spleen suggesting effectiveness of CoQ10/LPNs gel in reduction of inflammatory infiltration leading to suppression of keratinocyte hyperplasia in IMQ-induced plaque psoriatic mouse model that simulates the clinical psoriasis. Commercial product of IMQ (Imiquad® (5% w/w)) was topically applied onto the ES and BS of Swiss albino mice for 5 consecutive days that resulted into development of psoriasis-like inflammatory skin condition characterized by dermal damage (rete ridges, acanthosis, hyperplasia, parakeratosis, inflammatory infiltrate etc.), liver damage (fibrosis) and spleen damage (undifferentiated white pulp and red pulp). For ES and BS (Scale bar = 50 µm at 40X magnification) arrow abbr. are as follow- Red: Dermis; Blue: Epidermis; Black: Inflammatory infiltrates; Dark green: Stratum Corneum; Pink: Capillary Proliferation; White: Hyperkeratosis; Fluorescent green: Parakeratosis; Yellow: Epidermal Hyperaplasia. For liver (Scale bar = 50 µm at 40X magnification) arrow abbr. are as follow- Orange: Inflammatory infiltrates; Black: Hepatocytes; Green: Central Vein; Red: Hepatocytes Degeneration. For spleen (Scale bar = 50 µm at 40X magnification) arrow abbr. are as follow- White: Red Pulp; Black: White Pulp.

score of groups treated with CoQ10 gel (0.06% w/w), CoQ10/LPNs gel (0.03% w/w) and CoQ10/LPNs gel (0.06% w/w) were found to be 3, 1 and 0, respectively, indicating reduce

Table 5.1: Improved total skin damage score of the right ear (ES) and back skin (BS) after topical application of CoQ10/LPNs gel compared to CoQ10 gel using IMQ-induced plaque psoriatic mice model.

Groups	Parakeratosis	Hyperkeratosis	Angiogenesis	Hyperplasia	Inflammatory Infiltrate	Suprapapillary thinning	Pustule of Kogoj	Munro microabscess	Total skin damage Score
Negative control (ES)	-	-	-	-	-	-	-	-	0
Negative control (BS)	-	-	-	-	-	-	-	-	0
Positive control (ES)	**	***	**	***	***	*	-	*	15
Positive control (BS)	**	***	**	***	**	*	*	-	14
CoQ10 gel (0.06% w/w) (ES)	*	**	*	**	**	-	-	-	8
CoQ10 gel (0.06% w/w) (BS)	*	**	*	**	**	-	-	-	8
CoQ10/LPNs gel (0.03% w/w) (ES)	-	*	*	*	*	-	-	-	4
CoQ10/LPNs gel (0.03% w/w) (BS)	-	*	*	*	*	-	-	-	4
CoQ10/LPNs gel (0.06% w/w) (ES)	-	-	-	-	*	-	-	-	1
CoQ10/LPNs gel (0.06% w/w) (BS)	-	-	-	-	*	-	-	-	1

BS- Back skin.
ES- Ear skin.
'-' indicate no damage.
'*' indicate slight damage.
** indicate modest damage.
'***' indicate considerable damage.

damage in LPNs treated groups Table 5.2. Topical application of IMQ results in splenomegaly

(enlargement in spleen size), resulting in rupture of splenocytes leading to intermixing of the red pulp (pink color) and white pulp (blue color) areas. The efficiency of treatment was dictated by marked improvement (distinguishable) in red pulp and white pulp areas as observed in the negative control group. Treatment with CoQ10/LPNs gel demonstrated marked improvement in the red pulp and white pulp areas of spleen compared to free CoQ10 gel Figure 5.8. The total pleen damage score for positive control, CoQ10 gel (0.06% w/w), CoQ10/LPNs gel (0.03% w/w) and CoQ10/LPNs gel (0.06% w/w) were found to be 3, 2, 1 and 0 respectively Table 5.2.

Table 5.2. Improved total liver and spleen damage score after topical application of CoQ10/LPNs gel compared to CoQ10 gel using IMQ-induced plaque psoriatic mice model.

Groups	Inflammatory infiltrates	Hepatocyte degeneration	Total liver damage Score	Lymphocytes depopulation	Total Spleen damage Score
Negative control	-	-	-	-	0
Positive control	***	**	5	***	3
CoQ10 gel (0.06% w/w)	**	*	3	**	2
CoQ10/LPNs gel (0.03% w/w)	-	*	1	*	1
CoQ10/LPNs gel (0.06% w/w)	-	-	-	-	-

'-' indicate no damage
'*' indicate slight damage
'**' indicate modest damage
'***' indicate considerable damage

Application of IMQ on the back skin causes severe inflammation, which is followed by keratinocyte hyperplasia with over-expression of Ki67 nucleoprotein (cell proliferation marker). It was observed that animals treated with CoQ10/LPNs gel showed a significantly lower Ki67 as compared to the free CoQ10 gel Figure 5.9.

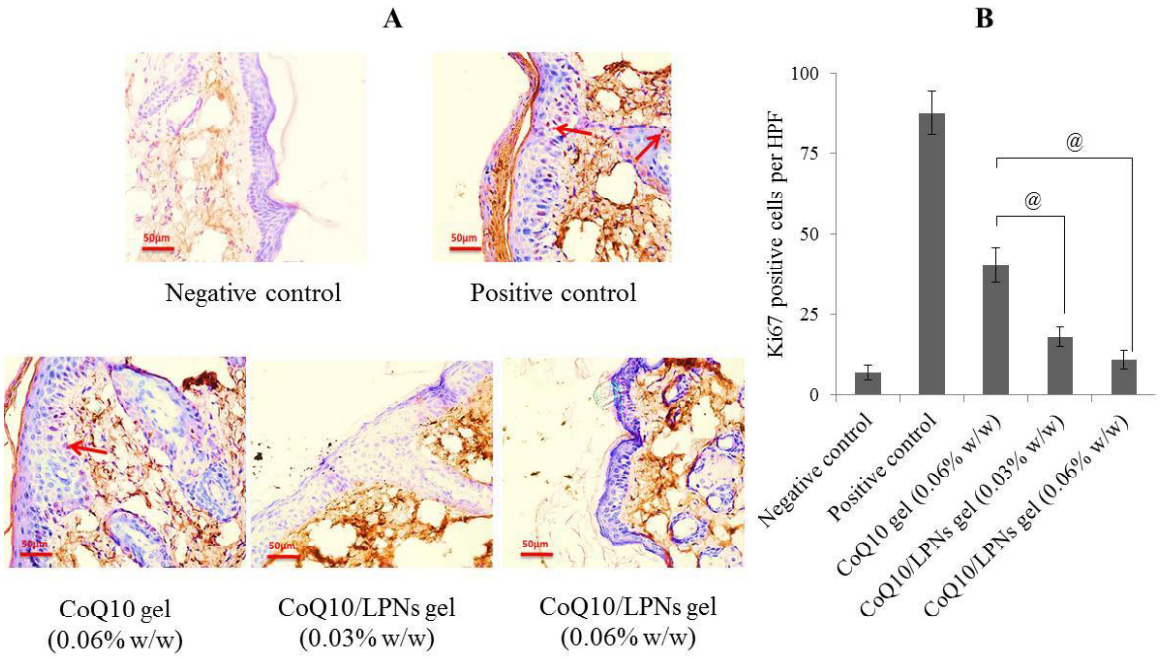

Figure 5.9. Ki67 (cell proliferating nucleoprotein) is found to be over-expressed in psoriatic lesions. (A) Immunohistochemical staining of Ki67 expressed in back skin of negative control or IMQ-induced psoriatic mice without or with treatment of CoQ10 containing formulations. CoQ10/LPNs gel resulted into significant reduction in expression of Ki67 which is over-expressed in psoriatic lesions. (Scale bar = 50 μm at 40X magnification). Red arrow signifies the higher expression of Ki67, (B) Graphs of average keratinocytes positive for Ki67 per High Power Field (HPF) of various groups indicated treatment with CoQ10/LPNs gel significantly reduced expression of cell proliferation marker and results were in alignment with the PASI scores. Data is presented as mean ± SD. #, $p \leq 0.05$ and @, $p \leq 0.01$, versus CoQ10 gel (0.06% w/w) treated group.

3.2.5. ROS scavenging efficacy

It is well established that oxidative stress exhibits a key role in the generation and progression of psoriatic inflammation. Therefore we evaluated the antioxidant efficacy of CoQ10 containing formulations using IMQ-induced psoriasis-like mice model by determining the levels of malondialdehyde (MDA) and glutathione (GSH). Figure 5.10, demonstrates that upon topical

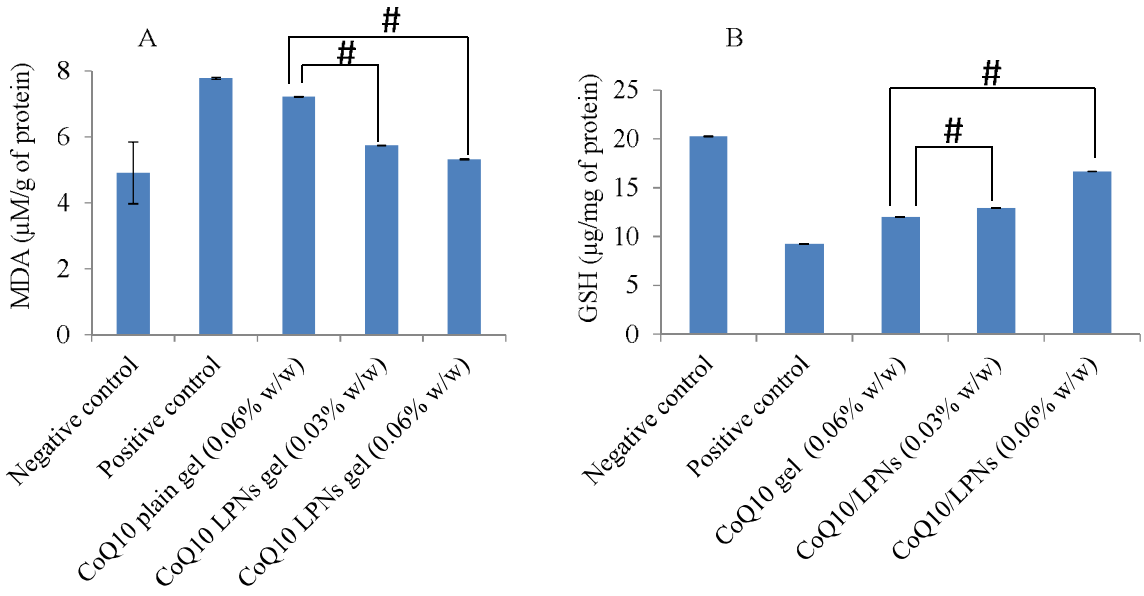

Figure 5.10. Comparative assessment of various groups w.r.t. (A) MDA and (B) GSH levels suggesting marked improvement in the antioxidant effect of CoQ10 when delivered as LPNs gel. Each value is represented as mean ± SD. #, $p < 0.001$ versus CoQ10 plain gel (0.06% w/w).

application of IMQ, MDA levels are markedly increased with a concomitant reduction in the bioactivity of GSH in comparison to the control group. In CoQ10/LPNs gels treated groups showed significant suppression of MDA levels with a concomitant increase in the levels of GSH compared to plain gel suggesting the significant improvement in the efficacy of the drug when delivered *via* lipid-polymer hybrid nano-particulate systems.

4. Discussion

Psoriasis is one of the most common chronic autoimmune dermatological disorders involving oxidative stress as one of the major underlying causes [10-15]. To combat the damage associated with ROS, skin is equipped with antioxidant defense systems (including enzymatic and non-enzymatic), and there should be a proper balance between the level of ROS and the defensive antioxidant system that ensures the maintenance of the integrity of the skin. In psoriasis, this balance is not retained due to the domination of pro-oxidants over skin self-defensive antioxidant mechanisms resulting in the generation of a higher level of ROS, causing cellular damage and inflammatory condition [14]. The currently available therapies for psoriasis suffer from severe drawbacks such as inapplicability for long-term usage because of associated toxicity issues [13]. It has been reported that the use of natural antioxidants in the management of this skin disease helps to restore the balance between pro-oxidant and antioxidant defense system with additionally supplemented with their long-term applicability due to lack of toxicity [2, 13, 16, 26-29].

It has been reported that CoQ10 supplementation improved the psoriatic condition [34]. It is highly lipophilic with log P value of 10 and enforces challenges for topical delivery. An ideal formulation of CoQ10 capable of penetrating deeper skin layers (viable epidermis and dermis where immune cells and keratinocytes interact as a result of ROS generation) with a sustained release profile (prevent rapid metabolism) is desirable. The nanoparticle (polymeric or lipidic) based approach is the preferred option, but both are associated with certain disadvantages over each other [43]. The advantages of lipid-polymer hybrid nanoparticles over both polymeric and lipidic systems are well reported, which includes high cellular uptake, better drug loading properties, a more controlled drug release behavior, and biocompatibility [43].

Our previously reported monolithic lipid-polymer hybrid nanoparticles-based platform technology for loading hydrophobic drugs was used for preparing CoQ10/LPNs. These earlier reported LPNs were found to substantially improve the intracellular uptake, exhibit deeper skin penetration into the viable dermal region, highly skin retentive properties releasing the drug in a sustained manner, and demonstrating a significantly improved *in vivo* anti-proliferative efficiency with a marked reduction in PASI scores [44]. FE-SEM image demonstrated CoQ10/LPNs possessed uniform and spherical morphology. LPNs showed a slow and sustained CoQ10 release profile due to the encapsulation of drug in the central hydrophobic core composed of solid lipid, liquid lipid and hydrophobic block of amphiphilic copolymer. These CoQ10/LPNs were formulated into topical hydrogel composed of carbopol 974P (0.75% w/w) (gelling agent), propylene glycol (humectant), propyl paraben and methyl paraben (preservative) and sodium hydroxide (pH adjusting agent).

Application of IMQ (Toll-like receptors (TLR) 7/8 agonist) on the right ear and back skin induces severe inflammation resulting in increased epidermal thickness due to underlying keratinocyte hyperplasia. *In vivo* antipsoriatic studies conducted on IMQ-induced psoriatic mouse model showed that test group treated with CoQ10/LPNs gel (0.06% w/w) showed significant improvement in PASI parameters, thickness (both back skin and ear) and average spleen weights compared to conventional gel i.e. CoQ10 gel (0.06% w/w). Even at half dose reduction i.e. 0.03% w/w, CoQ10/LPNs gel significantly improved all the above-aforementioned parameters compared to conventional gel i.e. CoQ10 gel (0.06% w/w). Further, in case of test group treated with CoQ10/LPNs gel (0.03% w/w), the spleen weights were found to be comparatively lower than groups treated with CoQ10 gel (0.06% w/w) indicating enhanced efficacy after formulating CoQ10 in LPNs system. Histopathological data proved that

CoQ10/LPNs gel treated group yield best results in reducing the total damage score of all the organs; skin (right ear and back skin), liver and spleen compared to conventional gel i.e. CoQ10 gel. Ki67 is a nucleoprotein reported to be highly expressed in proliferating cells and can serve as a marker for indicating the extent of cell proliferation. Psoriasis is characterized by hyperplasia of keratinocytes as a result of severe dermal inflammation leading to prominent increase in the epidermal thickness and is associated with over-expression of Ki67. The immunohistochemical (IHC) staining demonstrated significantly reduced expression of this cell proliferating marker in the group subjected to treatment with CoQ10/LPNs gel compared to conventional gel. This significant enhancement in the efficacy of CoQ10 after formulating into LPNs system might be credited to the improved dermal penetration, high cellular uptake with sustained drug release profile.

It is well established that oxidative stress exhibits a key role in the generation and progression of many skin diseases, including allergic contact dermatitis, psoriasis and atopic dermatitis. Therefore we evaluated the antioxidant efficacy of CoQ10 containing formulations using IMQ-induced psoriasis-like mice model by determining the levels of malondialdehyde (MDA) and glutathione (GSH). MDA is lipid peroxidation end product whose levels are towards higher side under oxidative stress condition whereas the GSH (biological antioxidant that are involved in suppressing the ROS) levels are reduced. It was observed that CoQ10/LPNs treatment increased the levels GSH, along with reduction in MDA formation to a significant extent compared to CoQ10 plain gel. These research findings suggested that CoQ10 could display greater antipsoriatic efficacy through antioxidant mechanisms when delivered as lipid-polymer hybrid nanoparticles.

5. Conclusion

Psoriasis is a chronic skin disease caused due to domination of pro-oxidants over skin's self-antioxidant defense system resulting in severe dermal inflammation. Present research employed an endogenous biomolecule CoQ10 with potent antioxidant and anti-inflammatory action for effective and long-term management of psoriasis. This endogenous molecule was delivered topically using monolithic lipid-polymer hybrid nanoparticles (CoQ10/LPNs) based platform technology that demonstrated deeper skin penetration with localized drug delivery. These CoQ10/LPNs demonstrated uniform spherical morphology with a sustained drug release profile. The *in-vivo* efficacy studies carried out using IMQ-induced plaque psoriatic mouse model suggested significant improvement in the efficacy of CoQ10 when delivered as LPNs, which can further serve as a platform for treating various dermatological diseases (cancer, acne, eczema etc.) and/or for cosmetic applications (skin whitening, anti-ageing, anti-wrinkle etc.)

References

[1] B. Limcharoen, P. Pisetpackdeekul, P. Toprangkobsin, P. Thunyakitpisal, S. Wanichwecharungruang, W. Banlunara, Topical Proretinal Nanoparticles: Biological Activities, Epidermal Proliferation and Differentiation, Follicular Penetration, and Skin Tolerability, ACS Biomater Sci Eng, 6(3) (2020), 1510-1521.

[2] M. Pleguezuelos-Villa, O. Diez-Sales, M.L. Manca, M. Manconi, A.R. Sauri, E. Escribano-Ferrer, A. Nácher, Mangiferin glycethosomes as a new potential adjuvant for the treatment of psoriasis, Int J Pharm, 573 (2020), 118844.

[3] C.H. Boakye, K. Patel, R. Doddapaneni, A. Bagde, S. Marepally, M. Singh, Novel amphiphilic lipid augments the co-delivery of erlotinib and IL36 siRNA into the skin for psoriasis treatment, J Control Release, 246 (2017), 120-132.

[4] A.M. Bowcock, J.G. Krueger, Getting under the skin: the immunogenetics of psoriasis, Nat Rev Immunol, 5(9) (2005), 699-711.

[5] R.J. Konrad, R.E. Higgs, G.H. Rodgers, W. Ming, Y.-W. Qian, N. Bivi, J.K. Mack, R.W. Siegel, B.J. Nickoloff, Assessment and clinical relevance of serum IL-19 levels in psoriasis and atopic dermatitis using a sensitive and specific novel immunoassay, Sci Rep, 9(1) (2019), 1-15.

[6] Y.S. Lee, M.-H. Lee, H.-J. Kim, H.-R. Won, C.-H. Kim, Non-thermal atmospheric plasma ameliorates imiquimod-induced psoriasis-like skin inflammation in mice through inhibition of immune responses and up-regulation of PD-L1 expression, Sci Rep, 7(1) (2017), 1-12.

[7] M.A. Lowes, A.M. Bowcock, J.G. Krueger, Pathogenesis and therapy of psoriasis, Nature, 445(7130) (2007), 866-873.

[8] J.U. Scher, A. Ogdie, J.F. Merola, C. Ritchlin, Preventing psoriatic arthritis: focusing on patients with psoriasis at increased risk of transition, Nat Rev Rheumatol, 15(3) (2019), 153-166.

[9] Y. Wang, R. Edelmayer, J. Wetter, K. Salte, D. Gauvin, L. Leys, S. Paulsboe, Z. Su, I. Weinberg, M. Namovic, Monocytes/Macrophages play a pathogenic role in IL-23 mediated psoriasis-like skin inflammation, Sci Rep, 9(1) (2019), 1-9.

[10] A.W. Armstrong, S.V. Voyles, E.J. Armstrong, E.N. Fuller, J.C. Rutledge, Angiogenesis and oxidative stress: common mechanisms linking psoriasis with atherosclerosis, J Dermatol Sci, 63(1) (2011), 1-9.

[11] H. Chen, C. Lu, H. Liu, M. Wang, H. Zhao, Y. Yan, L. Han, Quercetin ameliorates imiquimod-induced psoriasis-like skin inflammation in mice via the NF-κB pathway, Int Immunopharmacol, 48 (2017), 110-117.

[12] R. Darlenski, E. Hristakieva, U. Aydin, D. Gancheva, T. Gancheva, A. Zheleva, V. Gadjeva, J.W. Fluhr, Epidermal barrier and oxidative stress parameters improve during in 311 nm narrow band UVB phototherapy of plaque type psoriasis, J Dermatol Sci, 91(1) (2018), 28-34.

[13] P. Li, Y. Li, H. Jiang, Y. Xu, X. Liu, B. Che, J. Tang, G. Liu, Y. Tang, W. Zhou, Glabridin, an isoflavan from licorice root, ameliorates imiquimod-induced psoriasis-like inflammation of BALB/c mice, Int Immunopharmacol, 59 (2018), 243-251.

[14] Q. Zhou, U. Mrowietz, M. Rostami-Yazdi, Oxidative stress in the pathogenesis of psoriasis, Free Radic Biol Med, 47(7) (2009), 891-905.

[15] R. Lai, D. Xian, X. Xiong, L. Yang, J. Song, J. Zhong, Proanthocyanidins: novel treatment for psoriasis that reduces oxidative stress and modulates Th17 and Treg cells, Redox Rep, 23(1) (2018), 130-135.

[16] U. Mrowietz, J. Barker, W.H. Boehncke, L. Iversen, B. Kirby, L. Naldi, K. Reich, A. Tanew, P. van de Kerkhof, R. Warren, Clinical use of dimethyl fumarate in moderate-to-severe plaque-type psoriasis: a European expert consensus, J Eur Acad Dermatol Venereol, 32 (2018), 3-14.

[17] A.B. Gottlieb, Psoriasis: emerging therapeutic strategies, Nat Rev Drug Discov, 4(1) (2005), 19-34.

[18] M. Sala, A. Elaissari, H. Fessi, Advances in psoriasis physiopathology and treatments: Up to date of mechanistic insights and perspectives of novel therapies based on innovative skin drug delivery systems (ISDDS), J Control Release, 239 (2016), 182-202.

[19] O. Boyman, D. Comte, F. Spertini, Adverse reactions to biologic agents and their medical management, Nat Rev Rheumatol, 10(10) (2014), 612.

[20] M. Pradhan, D. Singh, M.R. Singh, Novel colloidal carriers for psoriasis: current issues, mechanistic insight and novel delivery approaches, J Control Release, 170(3) (2013), 380-395.

[21] M. Lebwohl, P. Ting, J. Koo, Psoriasis treatment: traditional therapy, Ann Rheum Dis, 64(suppl 2) (2005), 83-86.

[22] E.C. Murphy, S.W. Schaffter, A.J. Friedman, Nanotechnology for psoriasis therapy, Curr Dermatol Rep, 8(1) (2019), 14-25.

[23] A. Menter, C.E. Griffiths, Current and future management of psoriasis, Lancet, 370(9583) (2007), 272-284.

[24] S.C.-S. Hu, H.-S. Yu, F.-L. Yen, C.-L. Lin, G.-S. Chen, C.-C.E. Lan, Neutrophil extracellular trap formation is increased in psoriasis and induces human β-defensin-2 production in epidermal keratinocytes, Sci Rep, 6(1) (2016), 1-14.

[25] A. Jain, S. Doppalapudi, A.J. Domb, W. Khan, Tacrolimus and curcumin co-loaded liposphere gel: Synergistic combination towards management of psoriasis, J Control Release, 243 (2016), 132-145.

[26] B. Khurana, D. Arora, R.K. Narang, QbD based exploration of resveratrol loaded polymeric micelles based carbomer gel for topical treatment of plaque psoriasis: In vitro, ex vivo and in vivo studies, J Drug Deliv Sci Technol, 59 (2020), 101901.

[27] S. Sun, X. Zhang, M. Xu, F. Zhang, F. Tian, J. Cui, Y. Xia, C. Liang, S. Zhou, H. Wei, Berberine downregulates CDC6 and inhibits proliferation via targeting JAK-STAT3 signaling in keratinocytes, Cell Death Dis, 10(4) (2019), 1-16.

[28] S. Utaş, K. Köse, C. Yazici, A. Akdaş, F. Keleştimur, Antioxidant potential of propylthiouracil in patients with psoriasis, Clin Biochem, 35(3) (2002), 241-246.

[29] S. Zhang, X. Liu, L. Mei, H. Wang, F. Fang, Epigallocatechin-3-gallate (EGCG) inhibits imiquimod-induced psoriasis-like inflammation of BALB/c mice, BMC Complement Altern Med, 16(1) (2016), 1-11.

[30] Z. Xu, J. Huo, X. Ding, M. Yang, L. Li, J. Dai, K. Hosoe, H. Kubo, M. Mori, K. Higuchi, Coenzyme Q10 improves lipid metabolism and ameliorates obesity by regulating CaMKII-mediated PDE4 inhibition, Sci Rep, 7(1) (2017), 1-12.

[31] S. Jang, J. Lee, S.M. Ryu, H. Lee, J.-R. Park, H. Kim, D. Kim, A. Jang, S.-R. Yang, Effect of coenzyme Q10 via nitric oxide production and growth arrest of human colon cancer HCT116 cells, 예방수의학회지, 41(2) (2017), 59-65.

[32] D. Zhang, B. Yan, S. Yu, C. Zhang, B. Wang, Y. Wang, J. Wang, Z. Yuan, L. Zhang, J. Pan, Coenzyme Q10 inhibits the aging of mesenchymal stem cells induced by D-galactose through Akt/mTOR signaling, Oxid Med Cell Longev, (2015).

[33] Q. Zhao, Y.-M. Ma, L. Jing, T.-X. Zheng, H.-F. Jiang, P.A. Li, J.-Z. Zhang, Coenzyme Q10 protects astrocytes from ultraviolet B-induced damage through inhibition of ERK 1/2 pathway overexpression, Neurochem Res, 44(7) (2019), 1755-1763.

[34] Z. Kharaeva, E. Gostova, C. De Luca, D. Raskovic, L. Korkina, Clinical and biochemical effects of coenzyme Q10, vitamin E, and selenium supplementation to psoriasis patients, Nutrition, 25(3) (2009), 295-302.

[35] S.B. Lohan, S. Bauersachs, S. Ahlberg, N. Baisaeng, C.M. Keck, R.H. Müller, E. Witte, K. Wolk, S. Hackbarth, B. Röder, Ultra-small lipid nanoparticles promote the penetration of

coenzyme Q10 in skin cells and counteract oxidative stress, Eur J Pharm Biopharm, 89 (2015), 201-207.

[36] E.S. El-leithy, A.M. Makky, A.M. Khattab, Nanoemulsion formulations of nutraceutical coenzyme q10: preparation and evaluation for topical applications, 7 th International Scientific Conference of Faculty of Pharmacy Cairo University, (2016).

[37] E.S. EL-Leithy, A.M. Makky, A.M. Khattab, D.G. Hussein, Nanoemulsion gel of nutraceutical co-enzyme q10 as an alternative to conventional topical delivery system to enhance skin permeability and anti-wrinkle efficiency, Int J Pharm Pharm Sci, 9(11) (2017).

[38] E.S. El-Leithy, A.M. Makky, A.M. Khattab, D.G. Hussein, Optimization of nutraceutical coenzyme Q10 nanoemulsion with improved skin permeability and anti-wrinkle efficiency, Drug Dev Ind Pharm, 44(2) (2018), 316-328.

[39] E. Korkm, E.H. Gokce, O. Ozer, Development and evaluation of coenzyme Q10 loaded solid lipid nanoparticle hydrogel for enhanced dermal delivery, Acta Pharm, 63(4) (2013), 517-529.

[40] E.H. Gokce, E. Korkmaz, S. Tuncay-Tanrıverdi, E. Dellera, G. Sandri, M.C. Bonferoni, O. Ozer, A comparative evaluation of coenzyme Q10-loaded liposomes and solid lipid nanoparticles as dermal antioxidant carriers, Int J Nanomed, 7 (2012), 5109.

[41] W.-C. Lee, T.-H. Tsai, Preparation and characterization of liposomal coenzyme Q10 for in vivo topical application, Int J Pharm, 395(1-2) (2010), 78-83.

[42] K. Nayak, S.S. Katiyar, V. Kushwah, S. Jain, Coenzyme Q10 and retinaldehyde co-loaded nanostructured lipid carriers for efficacy evaluation in wrinkles, J Drug Targeting, 26(4) (2018), 333-344.

[43] T. Date, V. Nimbalkar, J. Kamat, A. Mittal, R.I. Mahato, D. Chitkara, Lipid-polymer hybrid nanocarriers for delivering cancer therapeutics, J Control Release, 271 (2018), 60-73.

[44] S.S. Pukale, S. Sharma, M. Dalela, A.K. Singh, S. Mohanty, A. Mittal, D. Chitkara, Multi-component clobetasol-loaded monolithic lipid-polymer hybrid nanoparticles ameliorate imiquimod-induced psoriasis-like skin inflammation in Swiss albino mice, Acta Biomater, 115 (2020), 393-409.

[45] J.-O. Baek, D. Byamba, W.H. Wu, T.-G. Kim, M.-G. Lee, Assessment of an imiquimod-induced psoriatic mouse model in relation to oxidative stress, Arch Dermatol Res, 304(9) (2012), 699-706.

[46] N.-W. Kang, M.-H. Kim, S.-Y. Sohn, K.-T. Kim, J.-H. Park, S.-Y. Lee, J.-Y. Lee, D.-D. Kim, Curcumin-loaded lipid-hybridized cellulose nanofiber film ameliorates imiquimod-induced psoriasis-like dermatitis in mice, Biomaterials, 182 (2018), 245-258.

[47] J.Y. Kim, J. Ahn, J. Kim, M. Choi, H. Jeon, K. Choe, D.Y. Lee, P. Kim, S. Jon, Nanoparticle-assisted transcutaneous delivery of a signal transducer and activator of transcription 3-inhibiting peptide Ameliorates psoriasis-like skin inflammation, ACS nano, 12(7) (2018), 6904-6916.

[48] Y. Chen, Q. Zhang, H. Liu, C. Lu, C.-L. Liang, F. Qiu, L. Han, Z. Dai, Esculetin ameliorates psoriasis-like skin disease in mice by inducing CD4+ Foxp3+ regulatory T cells, Front Immunol, 9 (2018), 2092.

[49] M. Xu, H. Lu, Y.-H. Lee, Y. Wu, K. Liu, Y. Shi, H. An, J. Zhang, X. Wang, Y. Lai, An interleukin-25-mediated autoregulatory circuit in keratinocytes plays a pivotal role in psoriatic skin inflammation, Immunity, 48(4) (2018), 787-798. e4.

[50] M. Ando, T. Kawashima, H. Kobayashi, A. Ohkawara, Immunohistological detection of proliferating cells in normal and psoriatic epidermis using Ki-67 monoclonal antibody, J Dermatol Sci, 1(6) (1990), 441-446.

[51] K. Nakajima, T. Kanda, M. Takaishi, T. Shiga, K. Miyoshi, H. Nakajima, R. Kamijima, M. Tarutani, J.M. Benson, M.M. Elloso, Distinct roles of IL-23 and IL-17 in the development of psoriasis-like lesions in a mouse model, J Immunol, 186(7) (2011), 4481-4489.

[52] R. Dou, Z. Liu, X. Yuan, D. Xiangfei, R. Bai, Z. Bi, P. Yang, Y. Yang, Y. Dong, W. Su, PAMs ameliorates the imiquimod-induced psoriasis-like skin disease in mice by inhibition of translocation of NF-κB and production of inflammatory cytokines, PLoS One, 12(5) (2017), e0176823.

[53] H.-L. Ha, H. Wang, P. Pisitkun, J.-C. Kim, I. Tassi, W. Tang, M.I. Morasso, M.C. Udey, U. Siebenlist, IL-17 drives psoriatic inflammation via distinct, target cell-specific mechanisms, Proc Natl Acad Sci, 111(33) (2014), E3422-E3431.

[54] G.M. Soliman, S.K. Osman, A.M. Hamdan, Preparation and evaluation of anthralin biodegradable nanoparticles as a potential delivery system for the treatment of psoriasis, Int J Pharm Pharm Sci, 7(12) (2015), 36-40.

[55] A. Zeb, F. Ullah, A simple spectrophotometric method for the determination of thiobarbituric acid reactive substances in fried fast foods, J Anal Methods Chem, (2016).

[56] I. Rahman, A. Kode, S.K. Biswas, Assay for quantitative determination of glutathione and glutathione disulfide levels using enzymatic recycling method, Nat Protoc, 1(6) (2006), 3159.